Supplementary materials for:

Cadmium Elimination via Magnetic Biochar Derived from Cow Manure: Parameter Optimization and Mechanism Insights

Yi Wen [1, 2], Dingxiang Chen [1, 2], Yong Zhang [1, 2], Huabin Wang [1, 2, *], and Rui Xu [1, 2, *]

[1] School of Energy and Environment Science, Yunnan Normal University, Kunming 650500, P. R. China; wyaquarius@foxmail.com (Y.W.); ynnuchendx@foxmail.com (D.C.); yongzhang7805@126.com (Y.Z.)

[2] Yunnan Key Laboratory of Rural Energy Engineering, Kunming 650500, P. R. China;

* Correspondence: E–mail address: hbwang@ynnu.edu.cn (H.W.); Tel: +86 27 65940928 (R.X.), Fax: +86 27 65940928 (R.X.), E–mail address: ecowatch_xr@163.com (R.X.).

Text S1. Calculation of adsorption capacity.

The removal rate of Cd(II) was calculated using Eq. 1. For the adsorption kinetics, the adsorption capacity of Cd(II) was calculated using Eq. 2. The experimental results were fitted using the adsorption dynamic model (Eq. 3, 4, 5, and 6).

$$\eta = \frac{(C_0 - C_e)}{C_0} \quad (1)$$

$$Q_e = (C_0 - C_e) \times \frac{V_0}{m} \quad (2)$$

$$Q_t = Q_e(1 - e^{-k_1 t}) \quad (3)$$

$$\frac{t}{Q_t} = \frac{1}{k_2 Q_e^2} + \frac{t}{Q_e} \quad (4)$$

$$Q_t = a + b\ln(t) \quad (5)$$

$$Q_t = K_{id} t^{0.5} + C \quad (6)$$

C_0 and C_e represent the mass concentration of Cd(II) at the initial and adsorption equilibrium in mg·g^{-1}, respectively; Q_e represents the adsorption capacity in mg·g^{-1}; V_0 is the volume of the Cd(II) solution (L); m represents the dosage of biochar in g; Q_t represents the adsorption capacity at time t in mg·L^{-1}; k_1 represents the reaction rate constant of the pseudo–first–order model (PFO) in min^{-1}; k_2 is the reaction rate constant of the pseudo–second–order model (PSO) in g·(mg·min)$^{-1}$; a and b are the initial adsorption rate and activation energy–related constants in mg·(g·min)$^{-1}$ and g·mg^{-1}, respectively; K_{id} is the intragranular diffusion rate constant in mg·(g·min$^{1/2}$)$^{-1}$; C is the boundary layer effect;

For isotherm studies, the experimental results were fitted using the isothermal adsorption model (Eq. 6 and Eq. 7)

$$Q_e = \frac{Q_m C_e K_L}{1 + K_L C_e} \quad (6)$$

$$Q_e = K_F C_e^{\frac{1}{n}} \quad (7)$$

In the equations, Q_e represents the adsorption capacity in mg·g^{-1}; C_e represents the mass concentration of Pb(II) in mg·L^{-1}; Q_m represents the theoretical maximum adsorption capacity in mg·g^{-1}; K_L represents the equilibrium constant of the Langmuir equation; K_F is the Freundlich constant, and n is the empirical constant.

Table S1. Variables and experimental conditions for RSM.

	Independent variables	Coded symbols	Levels		
			–1	0	1
Optimal synthesis parameters	Pyrolysis temperature (℃)	X_1	400	600	800
	Hydrothermal temperature (℃)	X_2	120	160	200
	Iron content (%)	X_3	5	10	15
	Adsorption quantity ($mg \cdot g^{-1}$)	Y		–	
Optimal reaction conditions	Dosage ($g \cdot L^{-1}$)	X_1	0.5	1.0	1.5
	pH	X_2	5	7	9
	Initial concentration ($mg \cdot L^{-1}$)	X_3	50	100	150
	Adsorption quantity ($mg \cdot g^{-1}$)	Y		–	

Table S2. BBD experimental design with the actual values of adsorption quantity with different biochar.

Run	X_1	X_2	X_3	Y
1	600	160	0.10	99.80
2	800	160	0.15	97.94
3	600	200	0.15	96.82
4	400	160	0.15	97.41
5	800	200	0.10	97.08
6	600	120	0.15	98.32
7	600	160	0.10	99.80
8	600	160	0.10	99.00
9	800	160	0.05	97.90
10	400	120	0.10	97.54
11	600	120	0.05	98.25
12	600	200	0.05	95.06
13	600	160	0.10	99.40
14	800	120	0.10	97.87
15	400	200	0.10	93.89
16	600	160	0.10	99.00
17	400	160	0.05	97.05

Table S3. ANOVA for response surface quadratic model.

Source	Sum of Squares	df	Mean Square	*F* Value	*p*–value Prob > F	
Model	37.51	9	4.17	19.70	0.0004	*significant*
X_1	10.41	1	10.41	49.23	0.0002	
X_2	3.00	1	3.00	14.19	0.0070	
X_3	0.62	1	0.62	2.93	0.1305	
$X_1 X_2$	2.04	1	2.04	9.64	0.0172	
$X_1 X_3$	0.71	1	0.71	3.37	0.1089	
X_2X_3	0.026	1	0.026	0.12	0.7360	
X_1^2	11.24	1	11.24	53.13	0.0002	
X_2^2	5.79	1	5.79	37.35	0.0012	
X_3^2	1.80	1	1.80	8.50	0.0225	
Residual	1.48	7	0.21			
Lack of Fit	0.84	3	0.28	1.75	0.2948	*not significant*
Pure Error	0.54	4	0.16			
Cor Total	38.99	16				

R–Squared: 0.9620; Adeq Precision: 14.950; C.V. %: 0.47%.

Table S4. BBD experimental design with the actual values of adsorption quantity under different reaction conditions

Run	X_1	X_2	X_3	Y
1	1.5	9	100	99.8
2	1	7	100	95.7
3	1.5	7	150	96.9
4	1.5	5	100	95.3
5	1	7	100	95.8
6	1	9	50	98
7	1	5	150	93.1
8	0.5	7	50	95.1
9	1.5	7	50	98.3
10	0.5	5	100	92.3
11	0.5	9	100	96.2
12	1	7	100	95.4
13	1	7	100	95.7
14	1	7	100	95.6
15	1	5	50	94.7
16	1	9	150	97.3
17	0.5	7	150	94.7

Table S5. ANOVA for response surface quadratic model.

Source	Sum of Squares	df	Mean Square	*F* Value	*p*–value Prob > F	
Model	53.13	9	5.90	102.15	< 0.0001	*significant*
X_1	18.00	1	18.00	311.50	< 0.0001	
X_2	31.60	1	31.60	546.87	< 0.0001	
X_3	2.10	1	2.10	36.36	0.0005	
$X_1 X_2$	0.090	1	0.090	1.56	0.2522	
$X_1 X_3$	0.25	1	0.25	4.33	0.0761	
X_2X_3	0.20	1	0.20	3.50	0.1034	
X_1^2	0.57	1	0.57	9.84	0.0164	
X_2^2	0.049	1	0.049	0.84	0.3893	
X_3^2	0.25	1	0.25	4.28	0.0772	
Residual	0.40	7	0.058			
Lack of Fit	0.31	3	0.10	4.53	0.0893	n*ot significant*
Pure Error	0.092	4	0.023			
Cor Total	53.53	16				

R–Squared: 0.9924; Adeq Precision: 37.832; C.V. %: 0.25%.

Table S6. Comparison of the statistical parameters of ANN and RSM models for the various responses.

		Optimum preparation conditions	Optimal reaction conditions
R^2	RSM	0.96	0.99
	ANN	0.98	0.99
RMSE	RSM	4.17	5.90
	ANN	1.13	1.02

Table S7. Fitting parameters of kinetic model and isotherm model of Cd(II) absorbtion.

Models	Parameters	TB
PFO	Q_e (mg·g^{-1})	99.2234
	k_1	1.2180
	R^2	0.9848
PSO	Q_e (mg·g^{-1})	104.8579
	K_2	0.0187
	R^2	0.9999
Elovich model	A (mg·g^{-1}·min^{-1})	69.93
	B (g·mg^{-1})	12.08
	R^2	0.7268
Internal diffusion model	K_{id1} mg·(g·min$^{1/2}$)$^{-1}$	50.80
	C (mg·g^{-1})	8.6288
	R^2	0.90503
	K_{id2} mg (g·min$^{1/2}$)$^{-1}$	0.4017
	C (mg·g^{-1})	97.7543
	R^2	0.3730
Langmuir model	Q_e (mg·g^{-1})	612.43
	K_L	1.14
	R^2	0.9956
Freundlich model	n	–0.02
	K_F	742.87
	R^2	0.9910

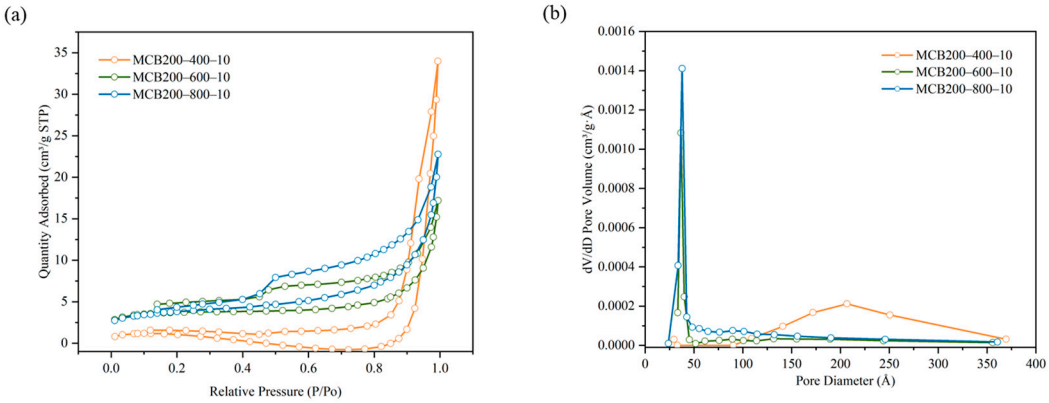


Figure S1. N_2 adsorption–desorption isotherms and pore size distribution curve.

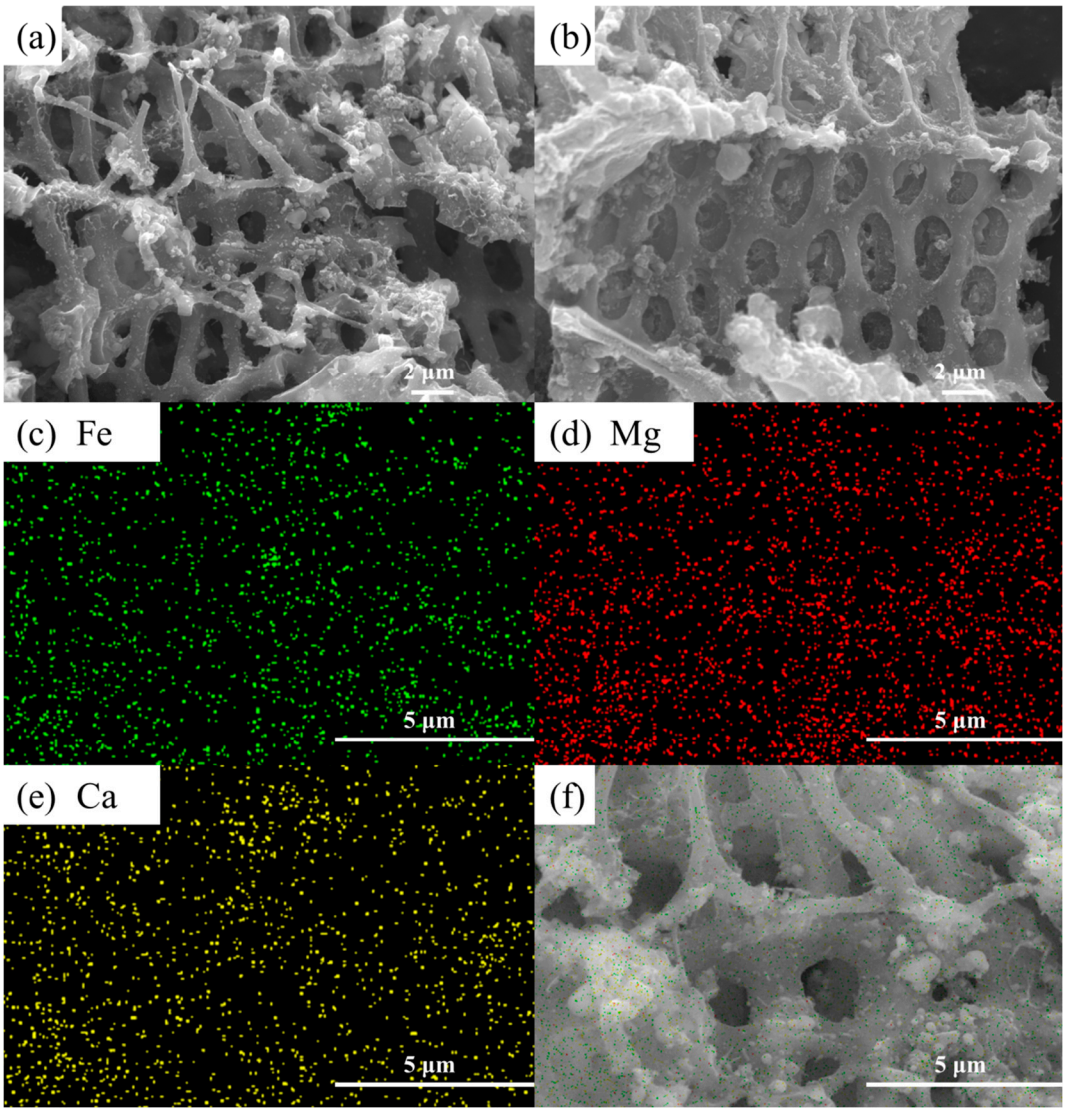


Figure S2. SEM (a and b) and SEM–EDS imagines of MCB (c – f).

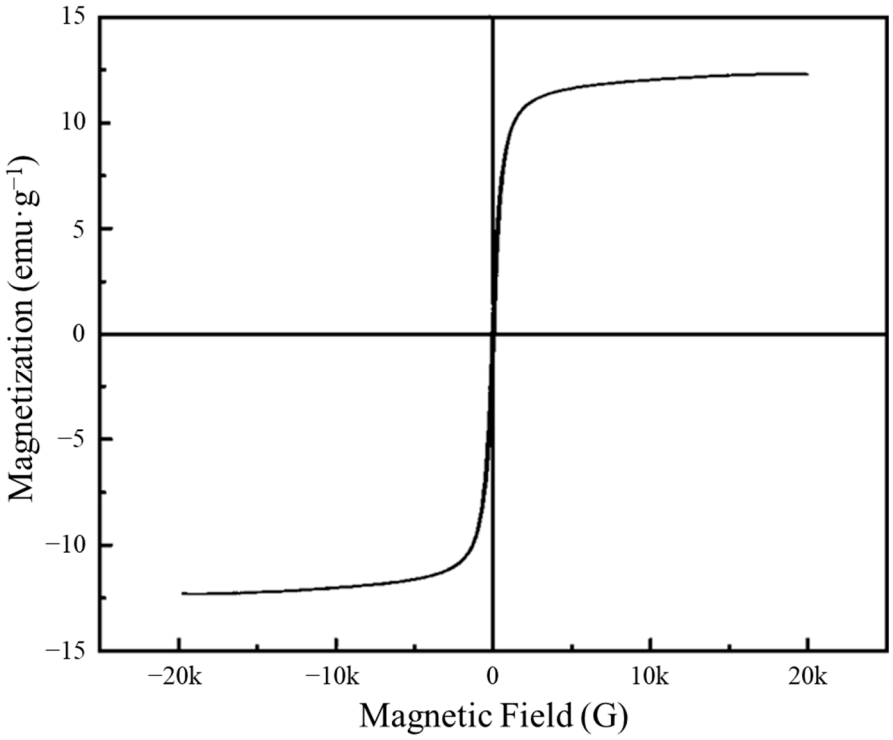


Figure S3. Magnetic hysteresis loop of MCB.

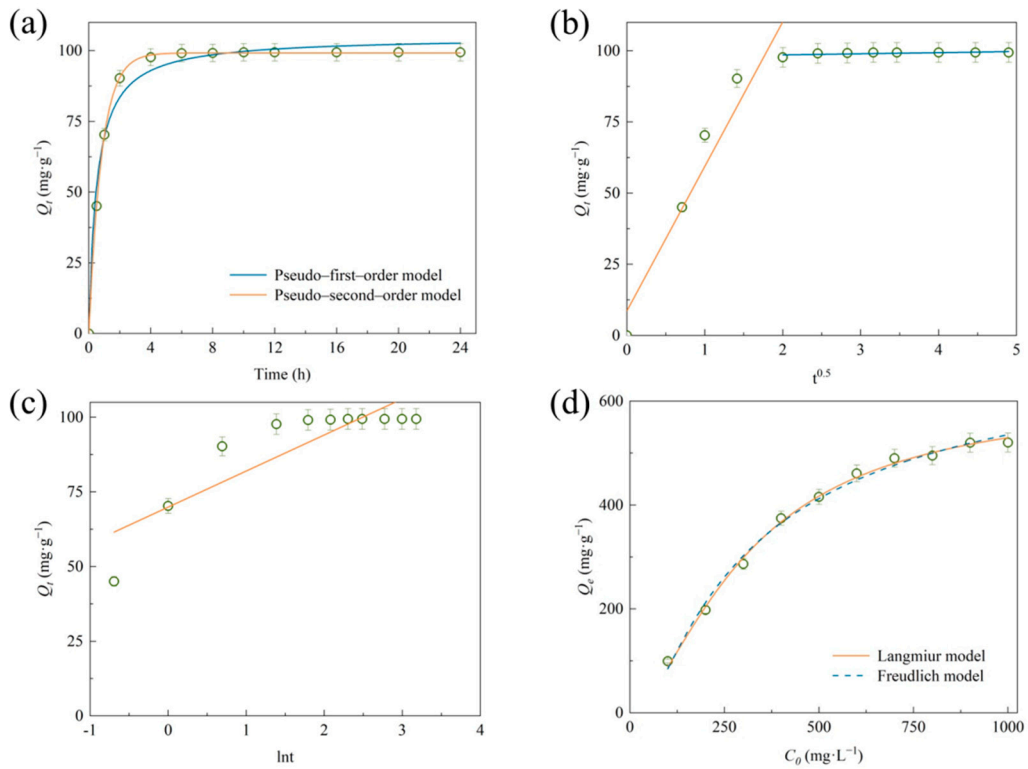


Figure S4. Fitting–figures of PFO, PSO (a), internal diffusion model (b), Elovich model (c), and isotherms (d) for the adsorption of Cd(II) on MCB. Experimental conditions: [initial concentration of Cd(II)] = 100 mg·L^{-1}, [dosage] = 1 g·L^{-1}, [time] = 24 h, [temperature] = 25 ℃.

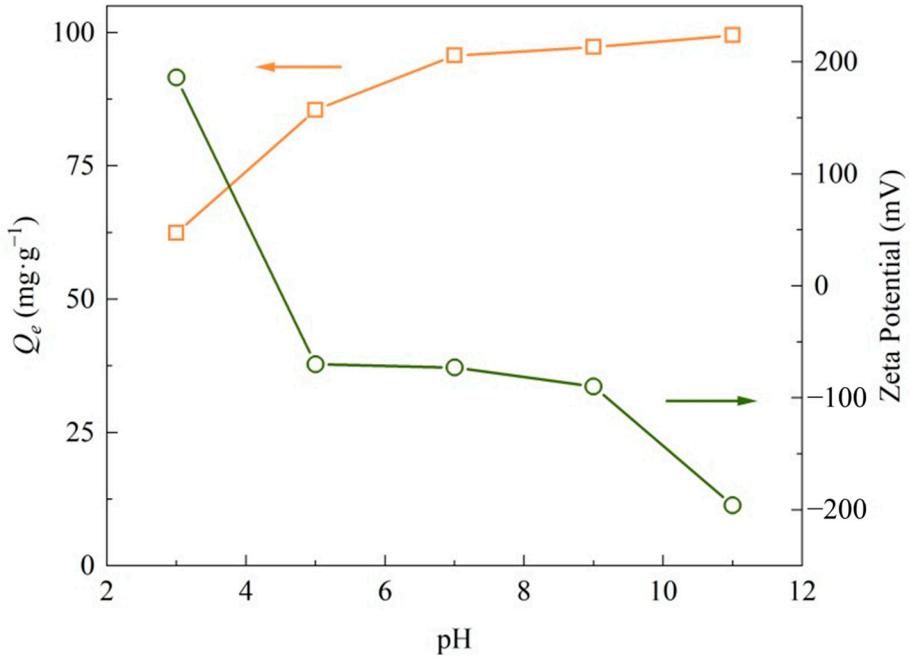


Figure S5. The effect of pH for adsorption Cd(II) by MCB. Experimental conditions: [initial concentration of Cd(II)] = 100 mg·L^{-1}, [dosage] = 1 g·L^{-1}, [time] = 24 h, [temperature] = 25 ℃.

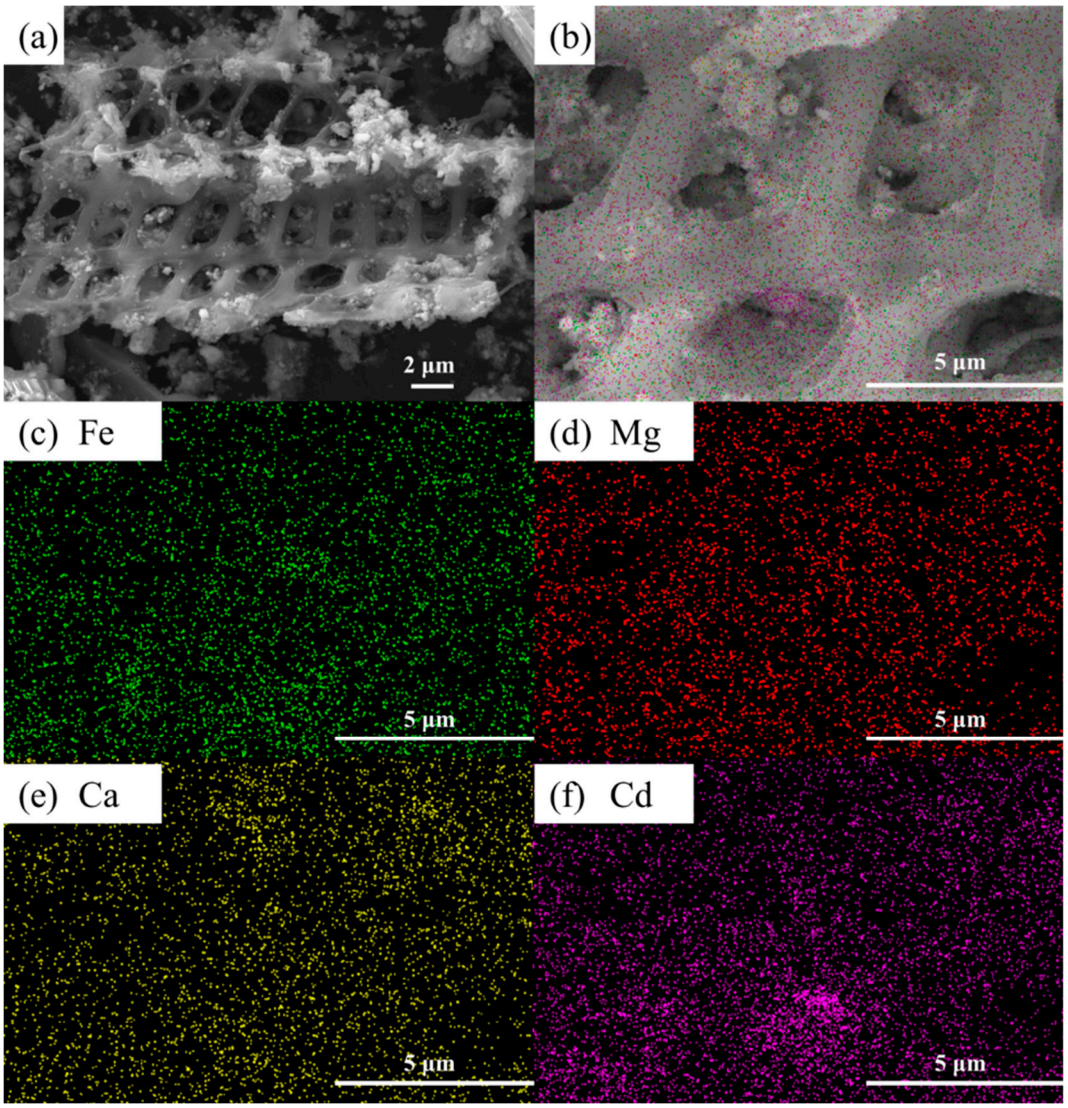


Figure S6. SEM–EDS imagines of Cd(II)–loaded MCB.

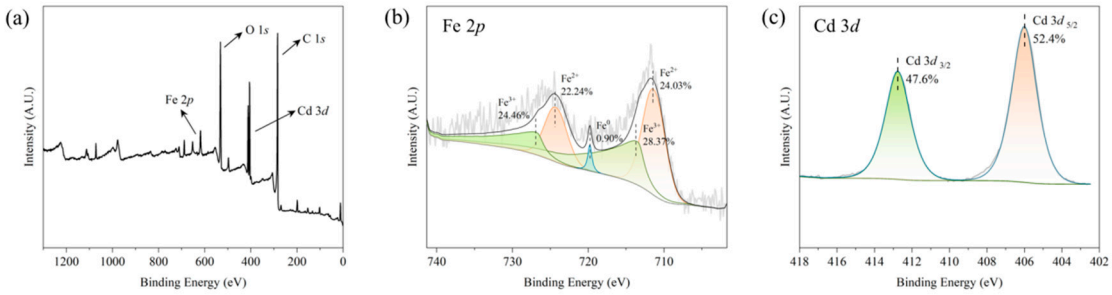


Figure S7. XPS spectrums of Cd(II)–loaded MCB.

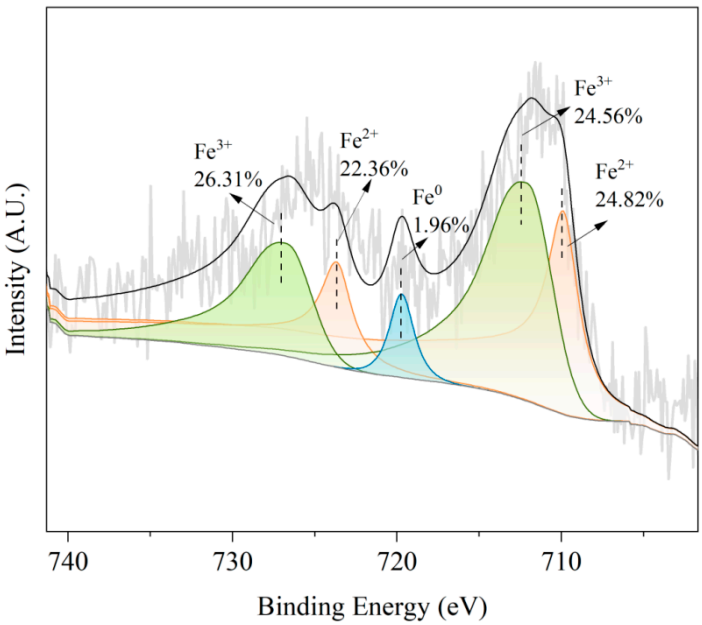


Figure S8. XPS Fe *2p* spectrum of MCB.